

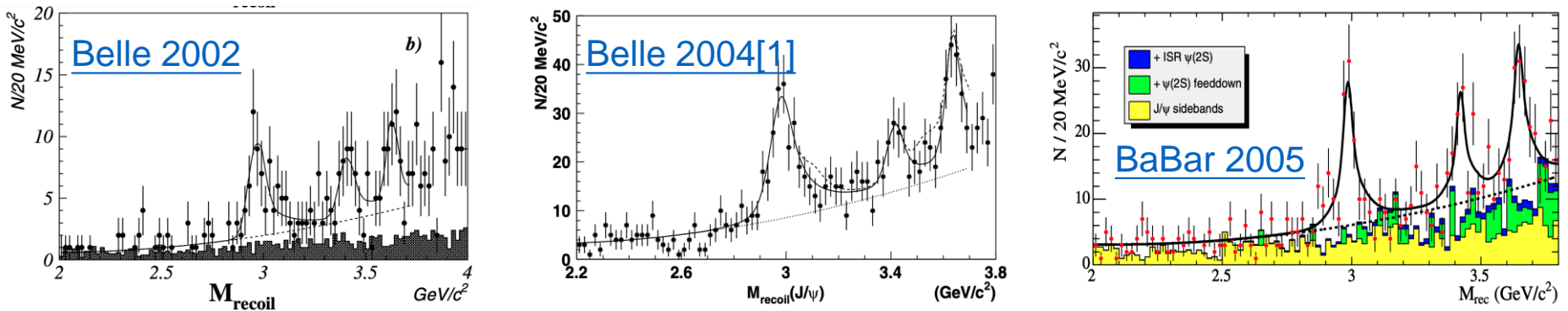
Study of $e^+e^- \rightarrow \phi + s\bar{s} + X$

Yuzhi Che, Yaquan Fang, Yanping Huang, Gang Li, Xinchou Lou,
Manqi Ruan, Jinfei Wu, **Gengyuan Zhang**, Huaqiao Zhang

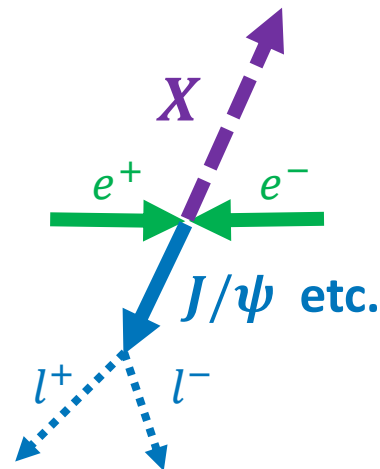
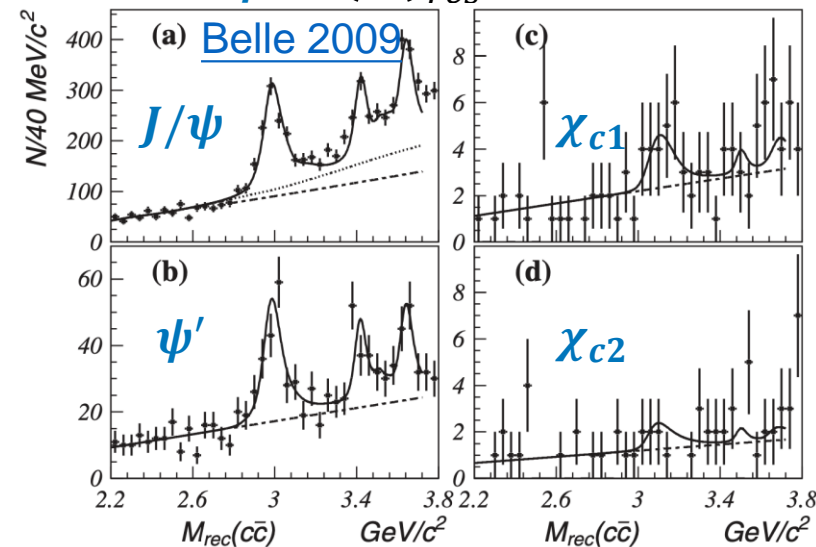
April 2nd, 2025

Motivation

- The significant double charmonium processes, $e^+e^- \rightarrow J/\psi + (c\bar{c})_{res}$, was observed by Belle, then confirmed by Belle and BaBar with higher significance.



- Except J/ψ , Belle also investigated the **other charmonium states** (tag side), such as $e^+e^- \rightarrow \psi' + (c\bar{c})_{res}$.

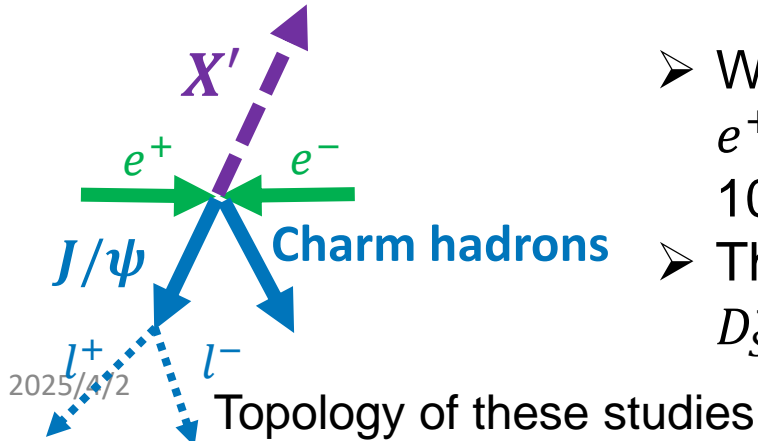
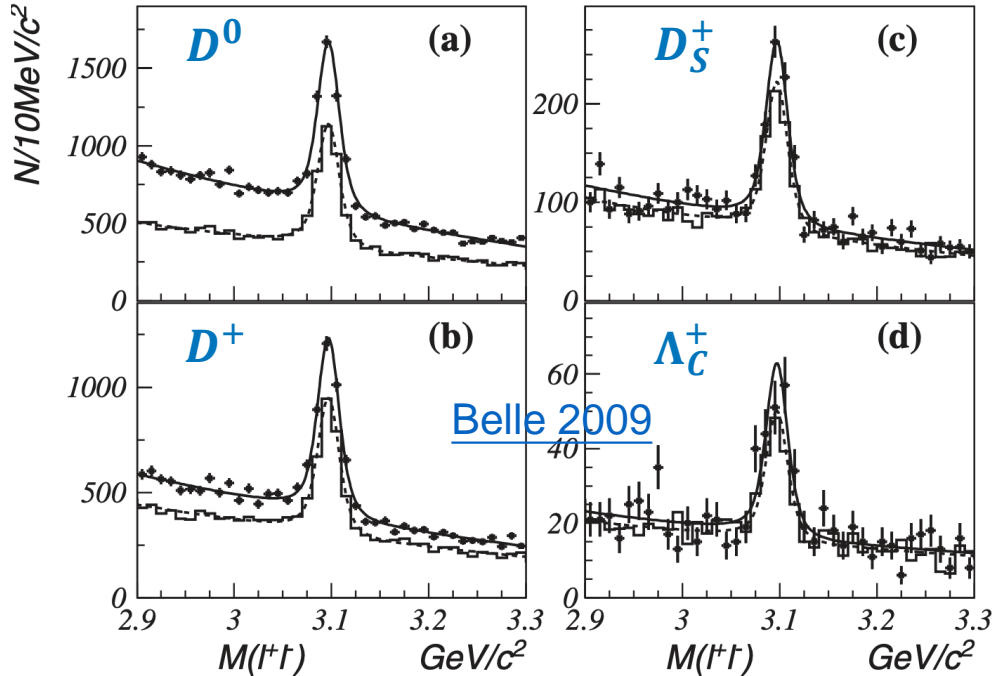
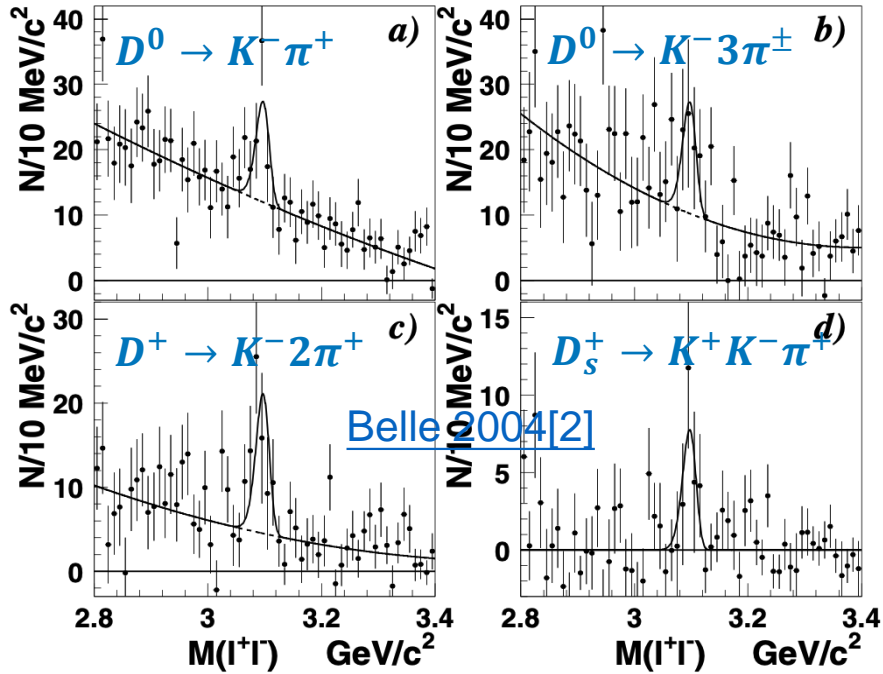


Topology of these studies

- Both Belle and BaBar had observed the significant double charmonium processes **below open charm**.

Motivation

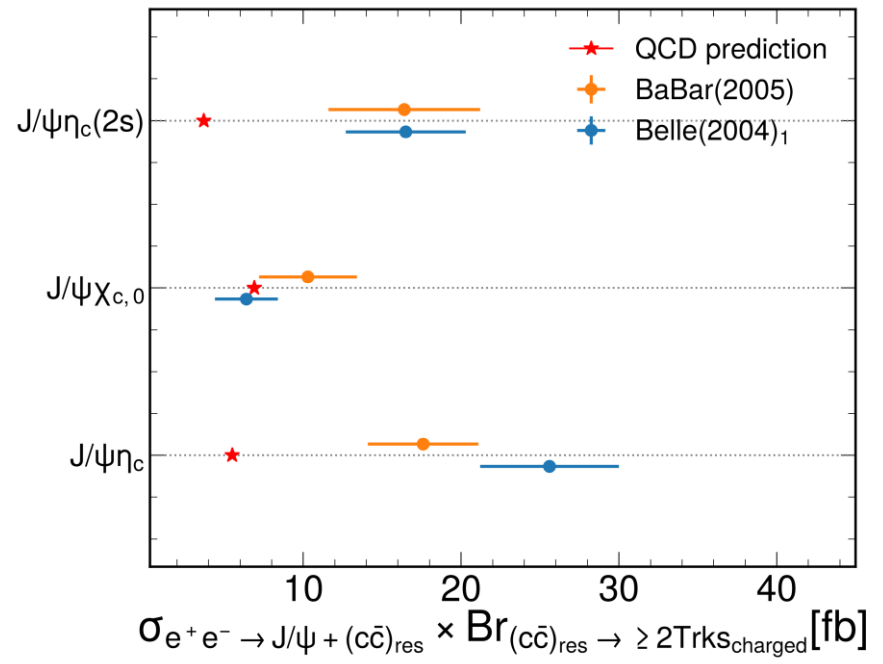
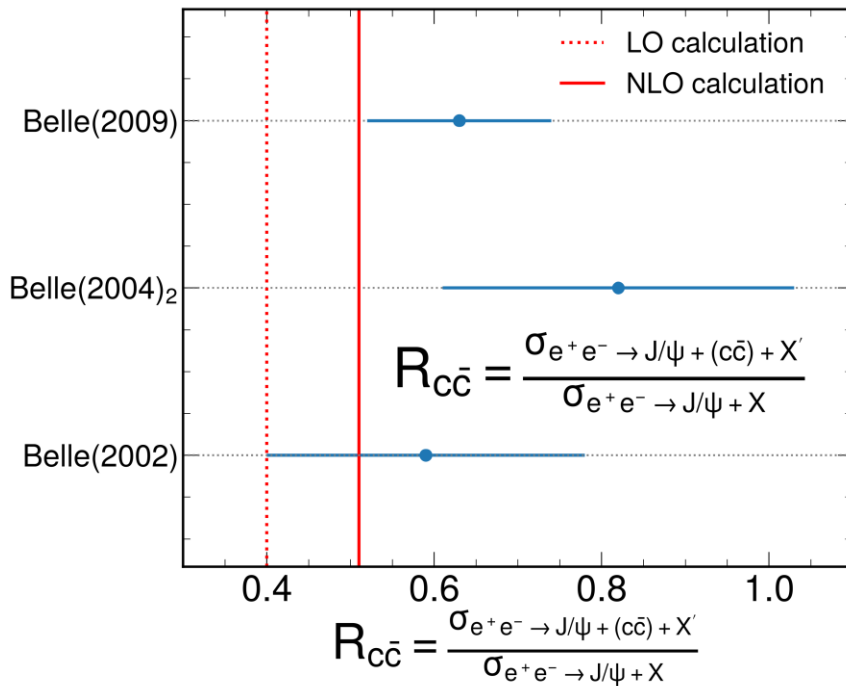
- The processes of $e^+e^- \rightarrow J/\psi + (c\bar{c})$ were also investigated **above open charm**.



- With more statistics, the significances of $e^+e^- \rightarrow J/\psi + D^0/D^+ + X'$ are improved to 10.1 and 7.8σ .
- The significances of $e^+e^- \rightarrow J/\psi + D_s^+/\Lambda_c^+ + X'$ are less than 5σ .

Motivation

- The experiment and QCD(NLO) have some discrepancy, especially in cross section ($3\sim 5\sigma$).



- The dominant mechanism for J/ψ production in e^+e^- annihilation is $e^+e^- \rightarrow J/\psi + c\bar{c}$.

Motivation

- We would like to perform studies with BESIII data to investigate the properties of strong interaction.
- BESIII had accumulated huge e^+e^- collision data from 2 to 4.95 GeV. Due to the lower C.M.S. energy, we cannot measure the double charmonium processes.
- So, we try to measure the double strangeonium processes, $e^+e^- \rightarrow \phi + s\bar{s} + X$ with BESIII data.
 - We will study the $e^+e^- \rightarrow \phi + s\bar{s} + X$ processes with the e^+e^- collision data@3.08GeV by measuring a ratio,

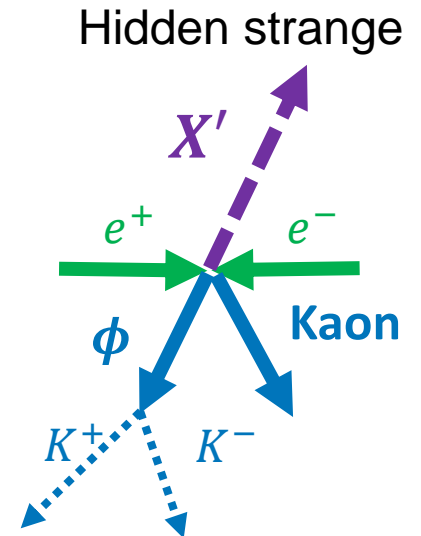
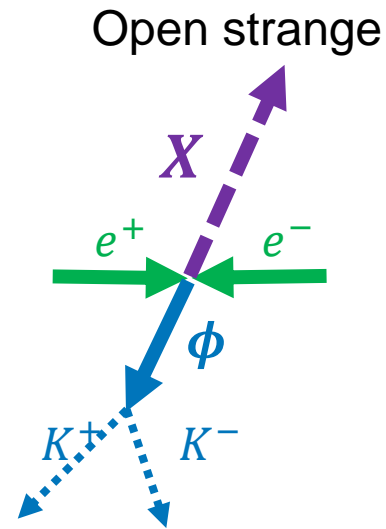
$$R_{s\bar{s}} = \frac{\sigma(e^+e^- \rightarrow \phi + (s\bar{s}) + X)}{\sigma(e^+e^- \rightarrow \phi + \text{anything})}$$

Methodology

➤ We investigate the $e^+e^- \rightarrow \phi + s\bar{s} + X$ processes in both hidden and open strange.

The following processes are taken into our account,

- $e^+e^- \rightarrow \phi + \eta$
- $e^+e^- \rightarrow \phi + K^+ + K^-$
- $e^+e^- \rightarrow \phi + K^+ + K^{*,-}$
- $e^+e^- \rightarrow \phi + K^- + K^{*,+}$
- $e^+e^- \rightarrow \phi + K^0/\bar{K}^0 + \bar{K}^0/K^0$
- $e^+e^- \rightarrow \phi + K^0/\bar{K}^0 + \bar{K}^{*,0}(K^{*,0})$



➤ The ϕ is reconstructed via $\phi \rightarrow K^+K^-$ decay mode, that gives better resolution.

Data and MC

- Boss version : 708.
- Data : e^+e^- collision data @3080 MeV.
- MC samples:
 - $e^+e^- \rightarrow \phi + \eta$
 - $e^+e^- \rightarrow \phi + K^+ + K^-$
 - $e^+e^- \rightarrow \phi + K^+ + K^{*,-}$
 - $e^+e^- \rightarrow \phi + K^- + K^{*,+}$
 - $e^+e^- \rightarrow \phi + K^0/\bar{K}^0 + \bar{K}^0/K^0$
 - $e^+e^- \rightarrow \phi + K^0/\bar{K}^0 + \bar{K}^{*,0}(K^{*,0})$

Event selection

- The event candidates are required to satisfy,
 - Good charged tracks **not originating from K_S^0** : $|R_{XY}| < 1\text{cm}$, $|R_Z| < 10\text{cm}$, $|\cos\theta| < 0.93$
 - Good charged tracks **originating from K_S^0** : $|\cos\theta| < 0.93$
 - Good photon : $0 \leq TDC \leq 14(50)\text{ns}$, $E_\gamma > 25/50 \text{ MeV}$ for $|\cos\theta| < 0.8 / 0.86 < |\cos\theta| < 0.92$
 - PID for pion/kaon/proton, $Prob(K) > Prob(\pi)$, $Prob(K) > Prob(p)$
 - K_S^0 reconstruction : secondary vertex fit is used, and a requirement on significance of decay length is applied.

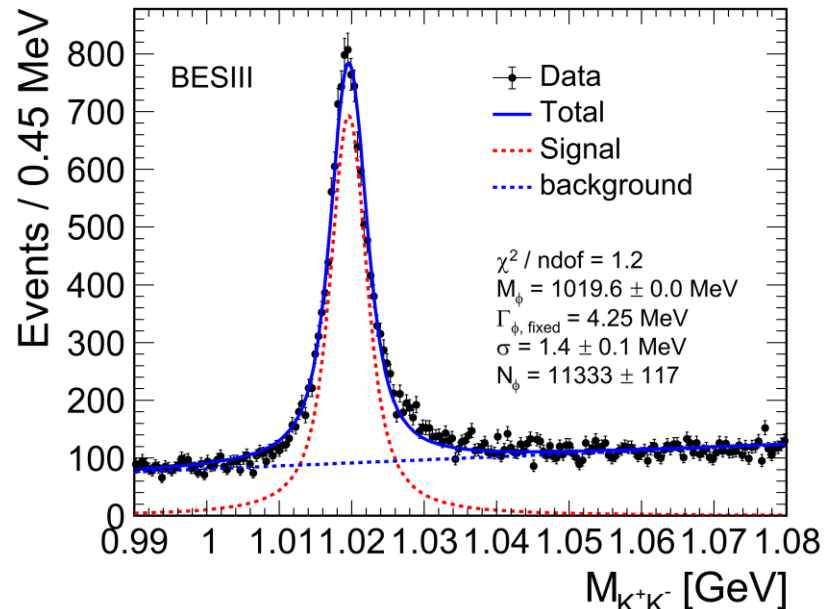
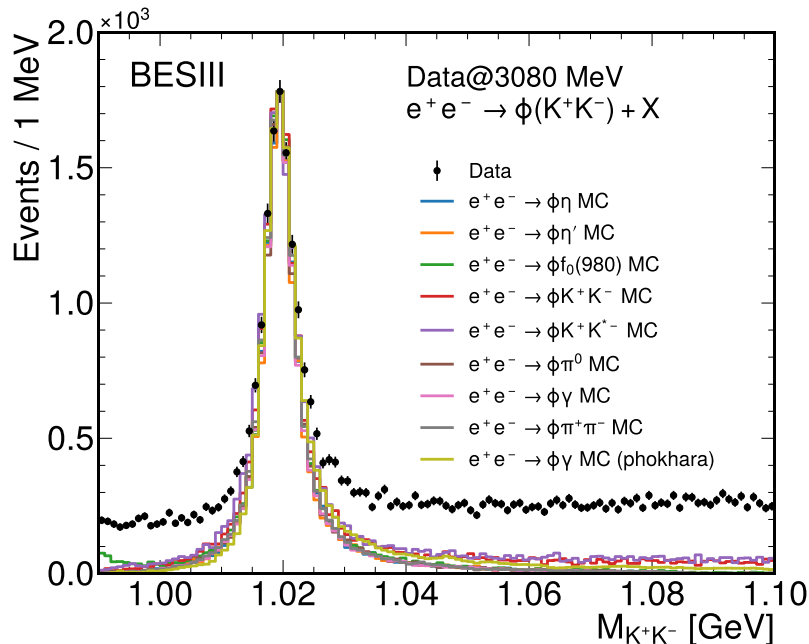
$$L/\sigma_L > 2$$

Event selection

- **Veto**s are applied to suppress possible backgrounds,
 - **At least 2 good charged tracks** with opposite charge, which are identified as a **pair of K^+K^-** .
 - All of the combinations of K^+K^- are used to reconstruct ϕ candidate.
- **Further selections on K_S^0 candidates** are applied to suppress possible backgrounds,
 - A pre-selection of K_S^0 candidate is adopted by requiring K_S^0 mass window, $M_{\pi^+\pi^-} \in [485, 515] \text{ MeV}$, $\sim 3\sigma$.

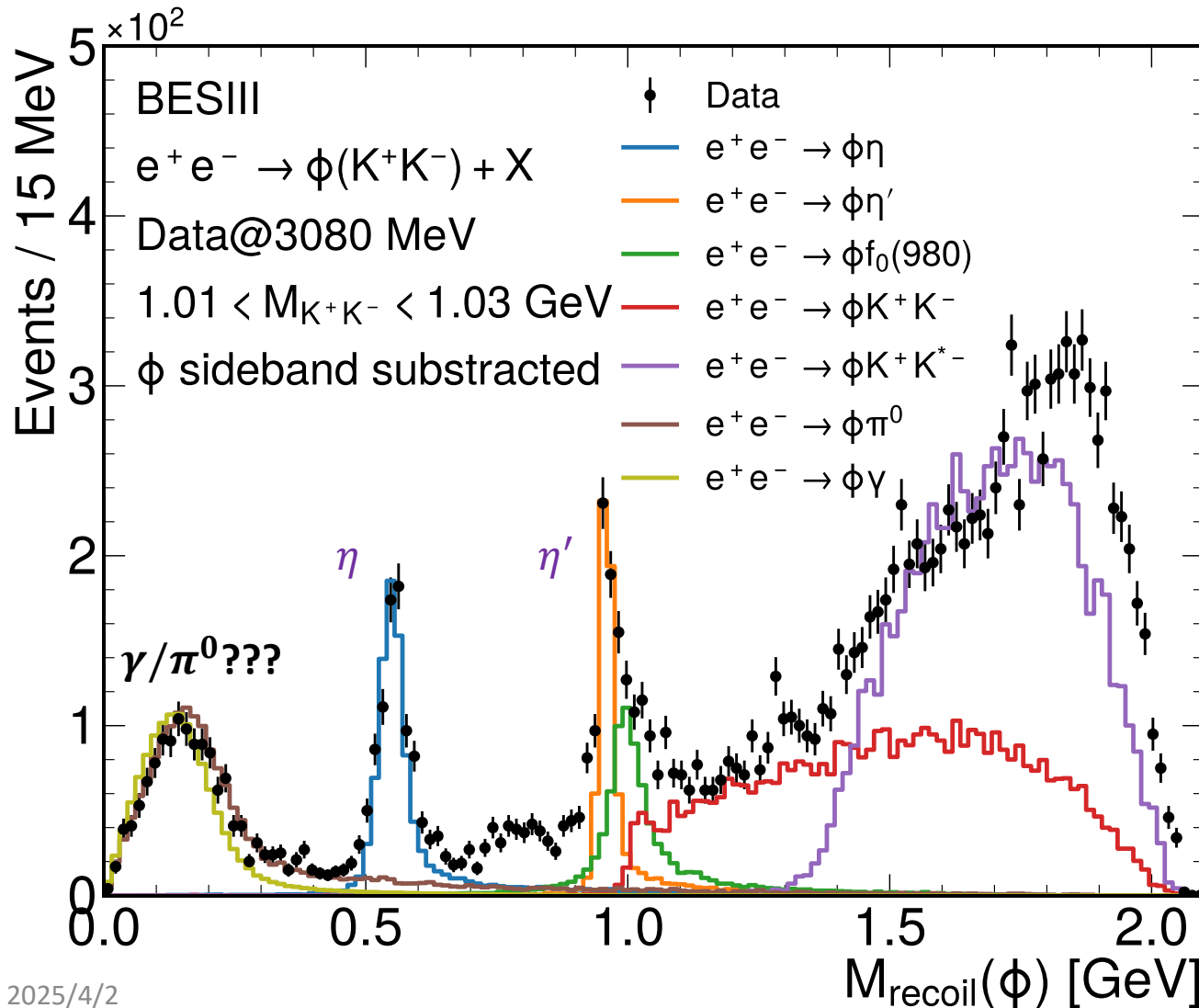
Event selection

- If there are more than 1 pair of K^+K^- passing the selection criteria, multiply entries will be stored.
- The signal mass window of ϕ is determined to be [1.01, 1.03] GeV.
 - The signal model is BW \otimes Double sides CB, and the background model is 2nd polynomial. The width of ϕ is fixed to PDG values.



The distribution of $M_{recoil}(\phi)$

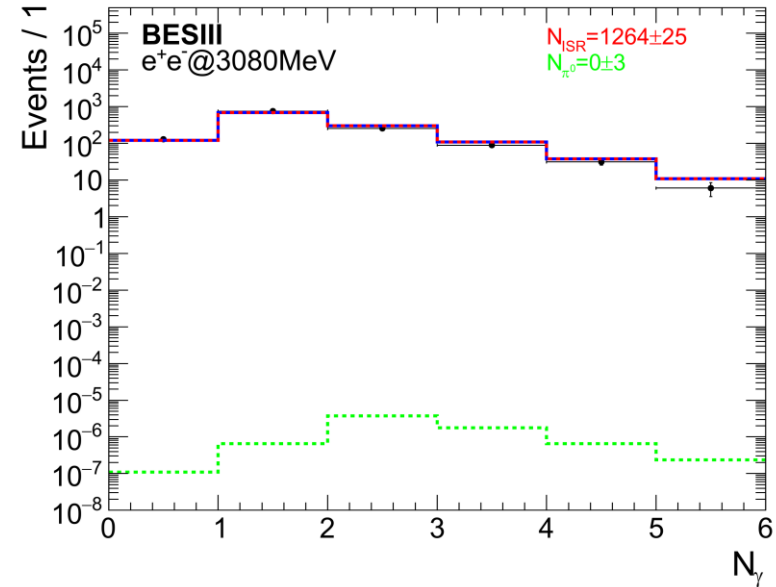
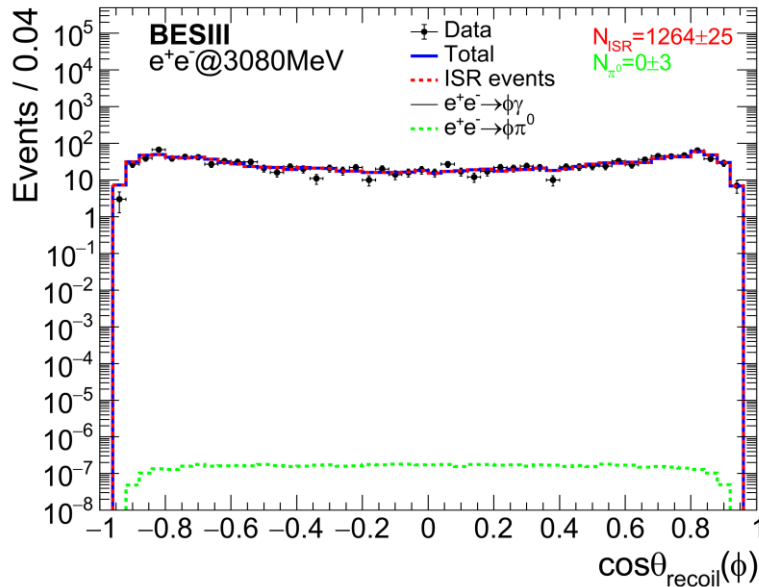
➤ The distribution of M_{recoil} against ϕ is shown in **data**.



Several clear peaks are observed, such as η , η' and f states.

Events in $M_{recoil}(\phi) < 0.4$ GeV region

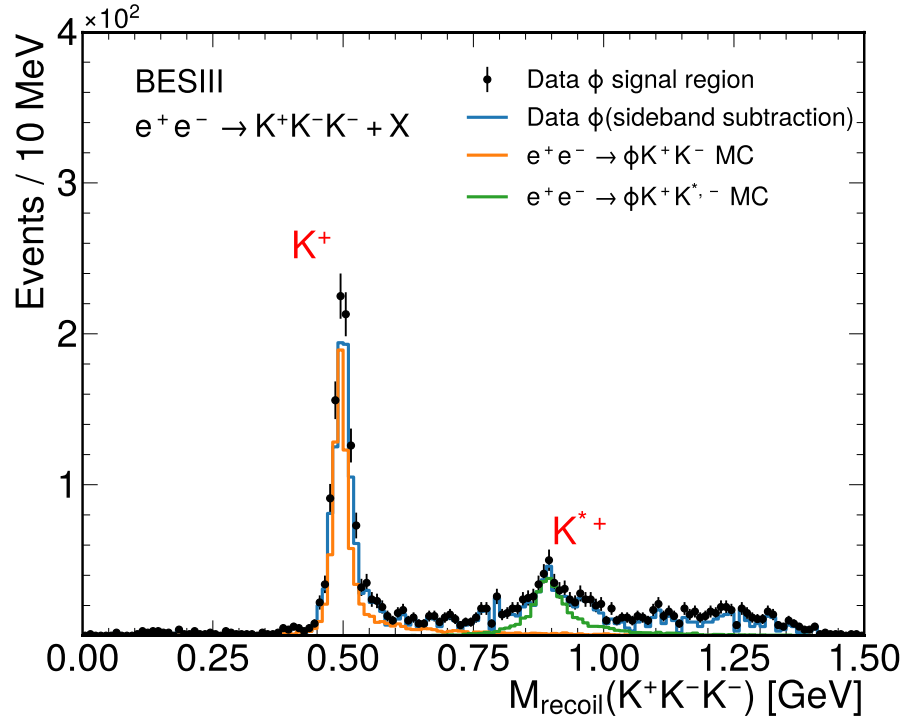
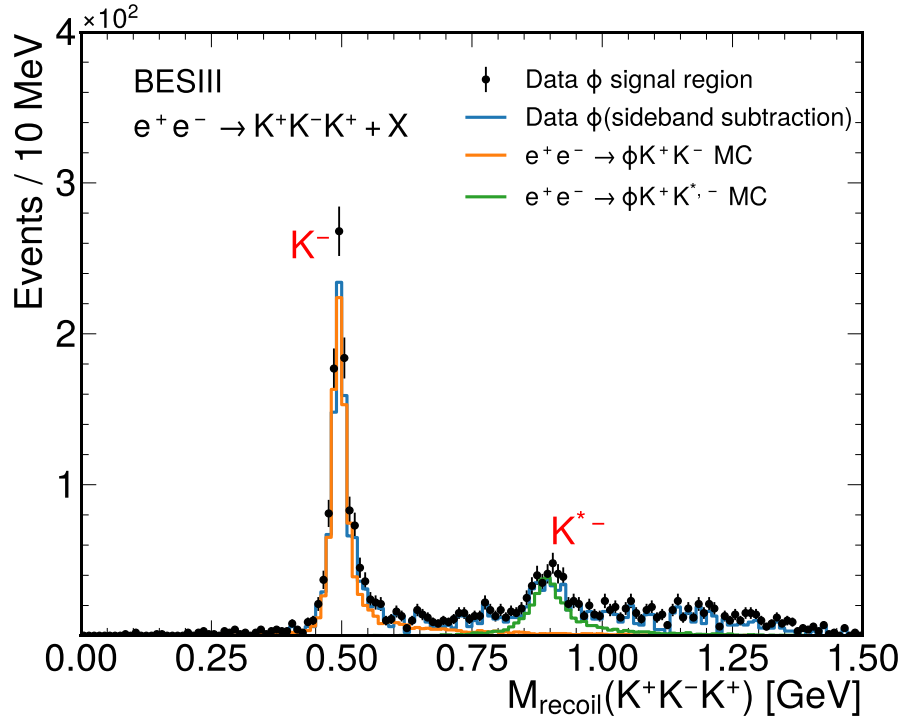
- The fit results of the simultaneous fit to N_γ and $\cos\theta_{recoil}(\phi)$.



- The Phokhara MC could also describe the data much better than the other MC sample.
- From the fit results, all of the photons are ISR photons.
- Because we focus on strong interaction part, the ISR process need to be removed.

DATA&MC comparison of $e^+e^- \rightarrow \phi K^\pm + X_1$

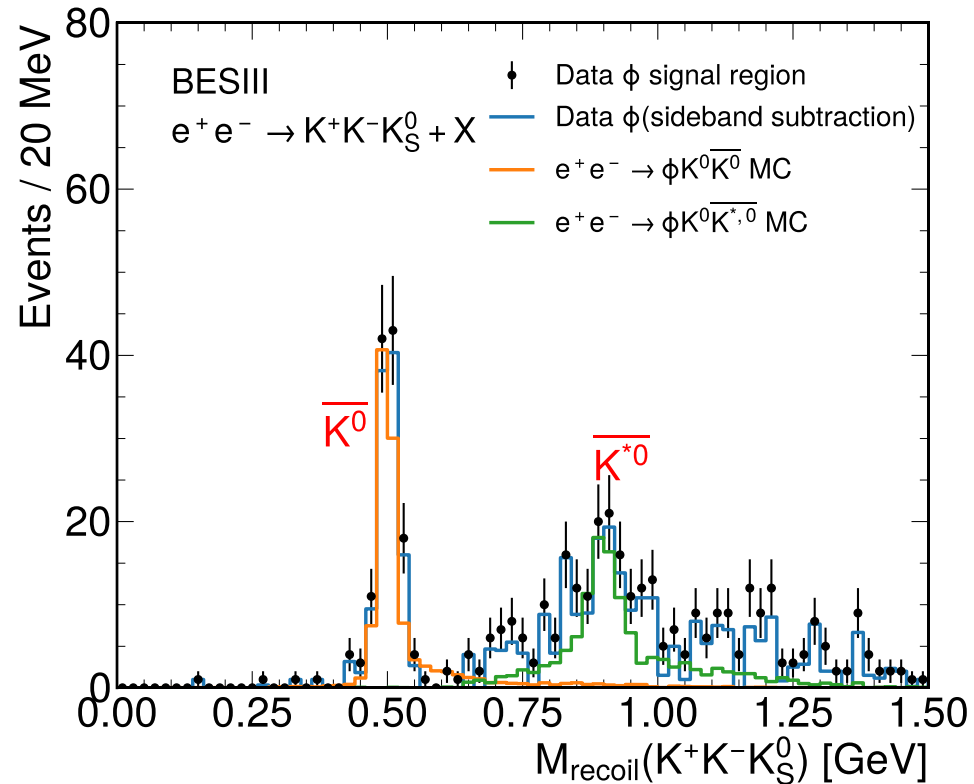
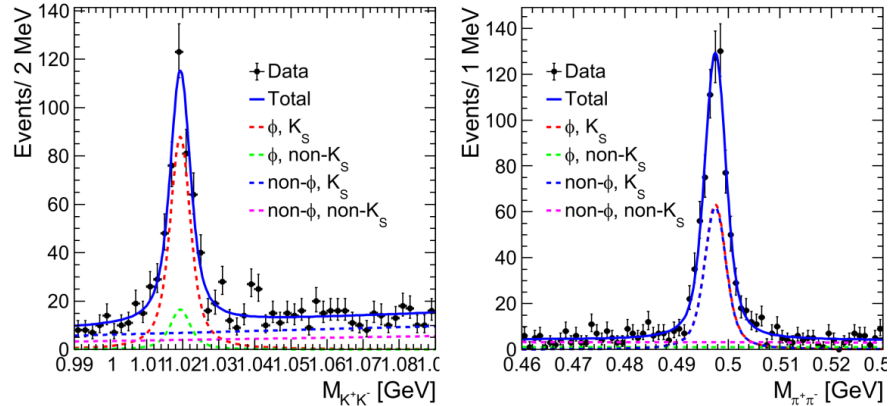
- The $K^\pm/K^{*,\pm}$ are observed in the distribution of M_{recoil} against $\phi + K^\mp$.
- From the inclusive MC studies, the possible backgrounds are only from **non- ϕ processes**, such as $e^+e^- \rightarrow K^+K^-K^+K^-$.



DATA&MC comparison of $e^+e^- \rightarrow \phi K_S^0 + X_2$

- The neutral kaon and K^* are observed in the distribution of M_{recoil} against $\phi + K_S^0$.
- The **non- K_S^0** and **non- ϕ** backgrounds are estimated by a 2D sideband method and subtracted in the recoil mass distribution.

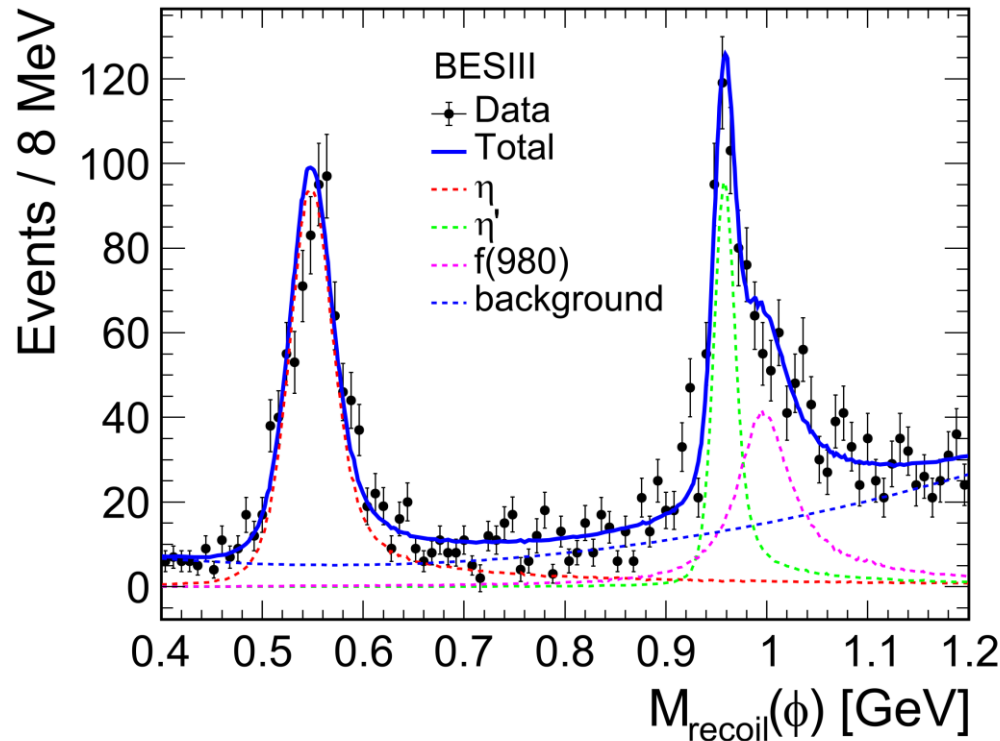
2D sideband method



Fit results of $M_{recoil}(\phi) < 1.2 \text{ GeV}$

➤ The distribution of M_{recoil} against ϕ is shown in **data**, and a mass spectrum fitting is performed to determine the number of events for $e^+e^- \rightarrow \phi + \eta$ and $e^+e^- \rightarrow \phi + \eta'$.

- MC shapes are used to describe the signal of η , η' and $f_0(980)$.

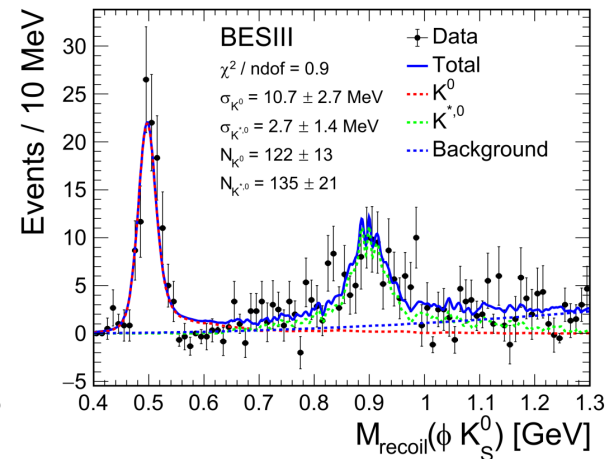
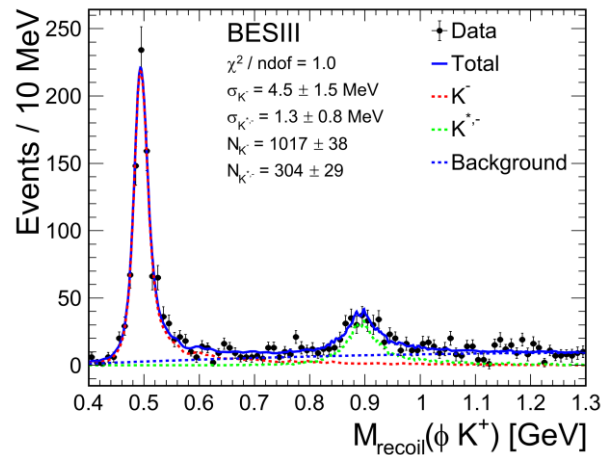
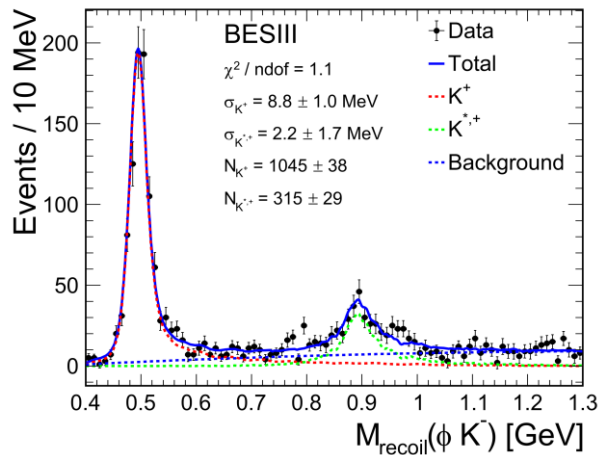


$$N_{\eta} = 877 \pm 39$$

$$N_{\eta'} = 435 \pm 33$$

Fit results of $M_{recoil}(\phi + K + X)$

- The fit results of M_{recoil} against ϕK^\pm and ϕK_S^0 , where the signal is described by MC shape \otimes gaussian and the background is described by 2nd order polynomial.
- The numbers of events for $e^+e^- \rightarrow \phi K^\pm K^\mp / K^{*,\mp}$, $e^+e^- \rightarrow \phi K_S^0 K_L^0 / K_S^0$ and $e^+e^- \rightarrow \phi K_S^0 K^{*,0} / \bar{K}^{*,0}$ are determined from the mass spectrum fitting.



Preliminary results

➤ The ratio ($R_{s\bar{s}} = \frac{\sigma(e^+e^- \rightarrow \phi + s\bar{s} + X')}{\sigma(e^+e^- \rightarrow \phi + X)}$) is calculated as

$$\begin{aligned}
 R_{s\bar{s}} &= \frac{\sigma(e^+e^- \rightarrow \phi + (s\bar{s}) + X)}{\sigma(e^+e^- \rightarrow \phi + \text{anything})} = \frac{N(e^+e^- \rightarrow \phi + (s\bar{s}) + X)}{N(e^+e^- \rightarrow \phi + \text{anything})} = \frac{\sum_i n_i(e^+e^- \rightarrow \phi + (s\bar{s}) + X_i)/\epsilon_i}{n(e^+e^- \rightarrow \phi + \text{anything})/\epsilon} \\
 &= \frac{\sum_i n_i(e^+e^- \rightarrow \phi + (s\bar{s}) + X_i)/(\epsilon_i/\epsilon)}{n(e^+e^- \rightarrow \phi + \text{anything})} = \frac{\sum_i n_i(e^+e^- \rightarrow \phi + X'_i)/\epsilon'_i \times f_i^{s\bar{s}}}{n(e^+e^- \rightarrow \phi + \text{anything})} \\
 &= \frac{\sum_i N_i(e^+e^- \rightarrow \phi + X'_i) \times f_i^{s\bar{s}}}{n(e^+e^- \rightarrow \phi + \text{anything})} = \frac{\sum_i N_i^{s\bar{s}}(e^+e^- \rightarrow \phi + X'_i)}{n(e^+e^- \rightarrow \phi + \text{anything})}
 \end{aligned}$$

➤ $n_i(e^+e^- \rightarrow \phi + X'_i)$ is the fitted number of events for the i th process.

➤ $\epsilon'_i = \frac{N_{\text{After all selection}}^i}{N_{\text{After selection of } \phi}^i}$ is the relative efficiency.

➤ $f_i^{s\bar{s}}$ is the fraction of $s\bar{s}$ components in the i th process.

Preliminary results

➤ The ratio ($R_{s\bar{s}} = \frac{\sigma(e^+e^- \rightarrow \phi + s\bar{s} + X')}{\sigma(e^+e^- \rightarrow \phi + X)}$) is determined to be $(38.4 \pm 1.4)\%$.

Table 3: The values of ϵ'_i , n_i , N_i , $f_i^{s\bar{s}}$, and $N_i^{s\bar{s}}$.

Process	ϵ'_i (%)	n_i	N_i	$f_i^{s\bar{s}}$	$N_i^{s\bar{s}}$
$e^+e^- \rightarrow \phi + \text{anything}$	1	11333 ± 117	11333 ± 117	-	-
$e^+e^- \rightarrow \phi + \gamma_{\text{ISR}}$	1	1264	1264	-	-
$e^+e^- \rightarrow \phi + \eta$	1	877 ± 39	877 ± 39	0.607 ± 0.006	533 ± 24
$e^+e^- \rightarrow \phi + \eta'$	1	435 ± 33	435 ± 33	0.794 ± 0.004	346 ± 26
$e^+e^- \rightarrow \phi K^+ + X(K^-)$	88.1 ± 0.8	1017 ± 38	1154 ± 44	1	1154 ± 44
$e^+e^- \rightarrow \phi K^+ + X(K^{*-})$	85.2 ± 0.9	304 ± 29	357 ± 34	1	357 ± 34
$e^+e^- \rightarrow \phi K^- + X(K^+)$	89.4 ± 0.8	1045 ± 38	1169 ± 44	1	1169 ± 44
$e^+e^- \rightarrow \phi K^- + X(K^{*-})$	86.3 ± 0.9	315 ± 29	365 ± 34	1	365 ± 34
$e^+e^- \rightarrow \phi K_S^0 + X(K_L^0/K_S^0)$	30.5 ± 0.4	122 ± 13	400 ± 43	1	400 ± 43
$e^+e^- \rightarrow \phi K_S^0 + X(K^{*,0}/\bar{K}^{*0})$	19.3 ± 0.4	135 ± 21	669 ± 110	1	669 ± 110

Systematic uncertainties

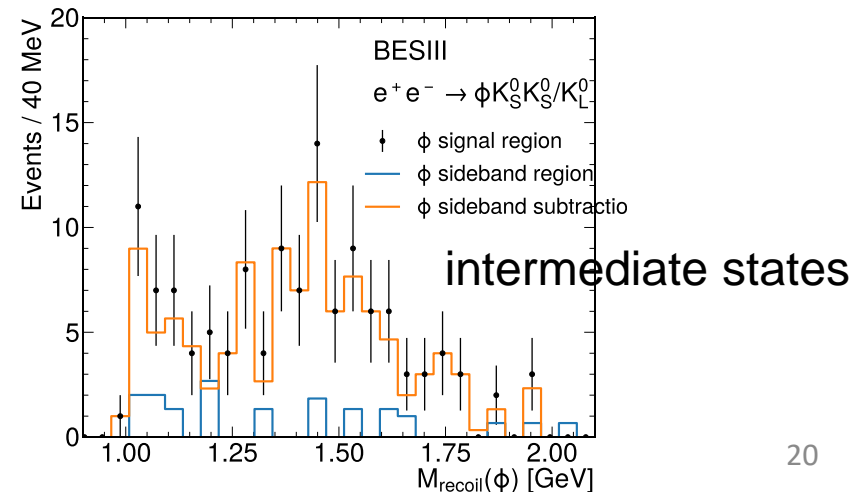
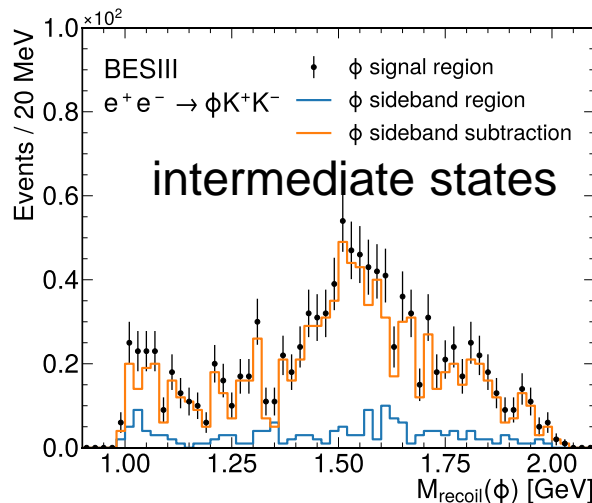
- Since we utilize relative efficiencies to determine the $R_{S\bar{S}}$, the systematic uncertainties related to ϕ selection are canceled.
- The remaining sources of systematic uncertainties are caused by
 - The detection and PID efficiency of additional K^\pm , 1% for each.
 - Reconstruction of K_S^0 , 1.5% per K_S^0 , [Ks systematic uncertainty](#)
 - Mis-modeling of MC is estimated by the difference of selection efficiency between the nominal and average of the MC samples with intermediate states.
 - Background description is estimated by changing the orders of polynomial functions.

Systematic uncertainties

➤ The systematic uncertainties caused by mis-modeling of MC are estimated

as

Process	ϵ_i	$\bar{\epsilon}$	Δ_ϵ
$e^+e^- \rightarrow \phi + f_0(980), f_0(980) \rightarrow K^+ + X(K^-)$	$(76.5 \pm 0.8)\%$	$(85.4 \pm 0.4)\%$	3.1%
$e^+e^- \rightarrow \phi + f_2(1270), f_2(1270) \rightarrow K^+ + X(K^-)$	$(88.2 \pm 0.9)\%$		
$e^+e^- \rightarrow \phi + f_0(1500), f_0(1500) \rightarrow K^+ + X(K^-)$	$(88.2 \pm 0.8)\%$		
$e^+e^- \rightarrow \phi + f_2'(1525), f_2'(1525) \rightarrow K^+ + X(K^-)$	$(88.8 \pm 0.9)\%$		
$e^+e^- \rightarrow \phi + f_0(980), f_0(980) \rightarrow K^- + X(K^+)$	$(78.2 \pm 0.8)\%$	$(86.5 \pm 0.4)\%$	3.2%
$e^+e^- \rightarrow \phi + f_2(1270), f_2(1270) \rightarrow K^- + X(K^+)$	$(88.9 \pm 0.9)\%$		
$e^+e^- \rightarrow \phi + f_0(1500), f_0(1500) \rightarrow K^- + X(K^+)$	$(89.3 \pm 0.8)\%$		
$e^+e^- \rightarrow \phi + f_2'(1525), f_2'(1525) \rightarrow K^- + X(K^+)$	$(89.4 \pm 0.8)\%$		
$e^+e^- \rightarrow \phi + f_0(980), f_0(980) \rightarrow K^0 \bar{K}^0$	$(29.7 \pm 0.4)\%$	$(30.7 \pm 0.2)\%$	0.7%
$e^+e^- \rightarrow \phi + f_2(1270), f_2(1270) \rightarrow K^0 \bar{K}^0$	$(31.1 \pm 0.4)\%$		
$e^+e^- \rightarrow \phi + f_0(1500), f_0(1500) \rightarrow K^0 \bar{K}^0$	$(30.8 \pm 0.4)\%$		
$e^+e^- \rightarrow \phi + f_2'(1525), f_2'(1525) \rightarrow K^0 \bar{K}^0$	$(31.3 \pm 0.4)\%$		
$e^+e^- \rightarrow K(1410)^{*, -} + X(K^{*, +}), K(1410)^{*, -} \rightarrow \phi K^-$	$(85.1 \pm 0.8)\%$	-	1.4%
$e^+e^- \rightarrow K(1410)^{*, +} + X(K^{*, -}), K(1410)^{*, +} \rightarrow \phi K^+$	$(84.5 \pm 0.8)\%$	-	0.8%
$e^+e^- \rightarrow K^{*, 0}(1410)/\bar{K}^{*, 0}(1410) + \bar{K}^{*, 0}/K^{*, 0},$ $K^{*, 0}(1410)/\bar{K}^{*, 0}(1410) \rightarrow \phi K^0/\bar{K}^0$	$(17.9 \pm 0.3)\%$	-	7.2%



Systematic uncertainties

➤ The systematic uncertainties caused by background description are

Table 6: The order of polynomial function in the recoil mass spectrum fitting.

Process	Order of nominal	Order of variation	Relative systematic uncertainty
$e^+e^- \rightarrow \phi + X(\text{anything})$	1	2	1.8%
$e^+e^- \rightarrow \phi + X(\eta)$	2	3	1.5%
$e^+e^- \rightarrow \phi + X(\eta')$	2	3	0.5%
$e^+e^- \rightarrow \phi + K^+ + X(K^-)$	2	3	0.8%
$e^+e^- \rightarrow \phi + K^+ + X(K^{*-})$	2	3	4.6%
$e^+e^- \rightarrow \phi + K^- + X(K^+)$	2	3	0.3%
$e^+e^- \rightarrow \phi + K^- + X(K^{*-})$	2	3	0.9%
$e^+e^- \rightarrow \phi + K_S^0 + X(K_L^0/K_S^0)$	2	3	0.0%
$e^+e^- \rightarrow \phi + K_S^0 + X(K^{*,0}/\bar{K}^{*0})$	2	3	11.8%

➤ The summary of systematic uncertainties are shown as below, which are less than the corresponding statistic uncertainty.

Process	Tracking	PID	K_S^0	Background	Efficiency	Total on $R_{s\bar{s}}$
$e^+e^- \rightarrow \phi + X(\text{anything})$	-	-	-	0.78%	-	0.78%
$e^+e^- \rightarrow \phi + X(\eta)$	-	-	-	0.08%	-	0.08%
$e^+e^- \rightarrow \phi + X(\eta')$	-	-	-	0.02%	-	0.02%
$e^+e^- \rightarrow \phi + K^+ + X(K^-)$	0.06%	0.06%	-	0.05%	0.18%	0.21%
$e^+e^- \rightarrow \phi + K^+ + X(K^{*-})$	0.04%	0.04%	-	0.16%	0.03%	0.17%
$e^+e^- \rightarrow \phi + K^- + X(K^+)$	0.06%	0.06%	-	0.02%	0.19%	0.21%
$e^+e^- \rightarrow \phi + K^- + X(K^{*-})$	0.04%	0.04%	-	0.03%	0.05%	0.08%
$e^+e^- \rightarrow \phi + K_S^0 + X(K_L^0/K_S^0)$	-	-	0.06%	0.00%	0.03%	0.07%
$e^+e^- \rightarrow \phi + K_S^0 + X(K^{*,0}/\bar{K}^{*0})$	-	-	0.10%	0.82%	0.50%	0.97%

Summary

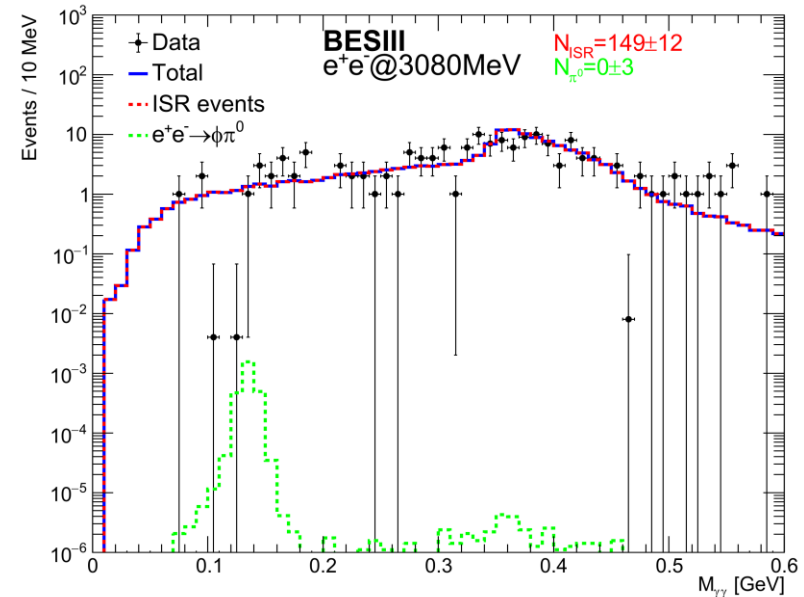
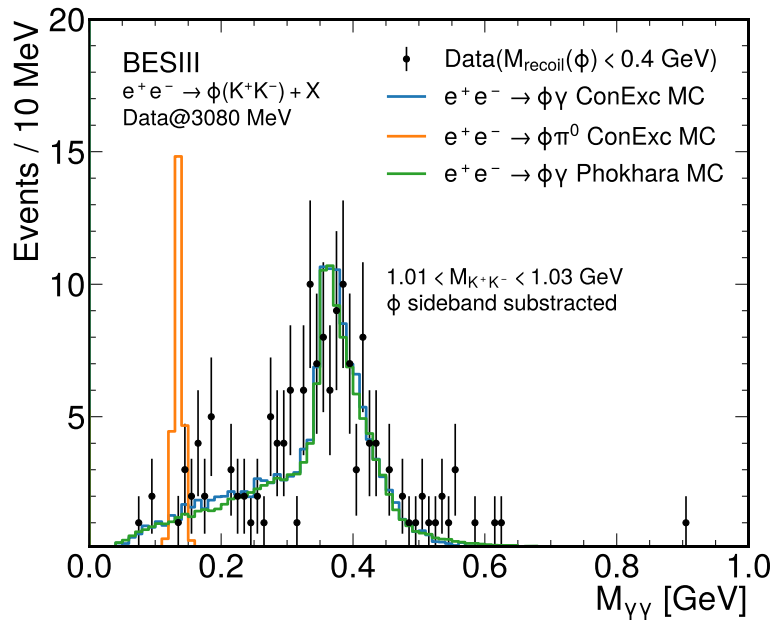
- Using 167pb^{-1} data @3080 MeV, we study $ee \rightarrow \phi + s\bar{s} + X$ processes and measure the $R_{s\bar{s}}$.
- Currently, $R_{s\bar{s}}$ is determined to be $(38 \pm 1.4_{stat} \pm 1.3_{syst})\%$ by considering $s\bar{s} + X$ as KK, KK^*, η and η' .
- In future studies, we will include more processes of $s\bar{s} + X$ to calculate $R_{s\bar{s}}$.
- Memo is ready.

Thanks for attention!

Backup

$M_{\gamma\gamma}$ in $M_{recoil}(\phi) < 0.4$ GeV region

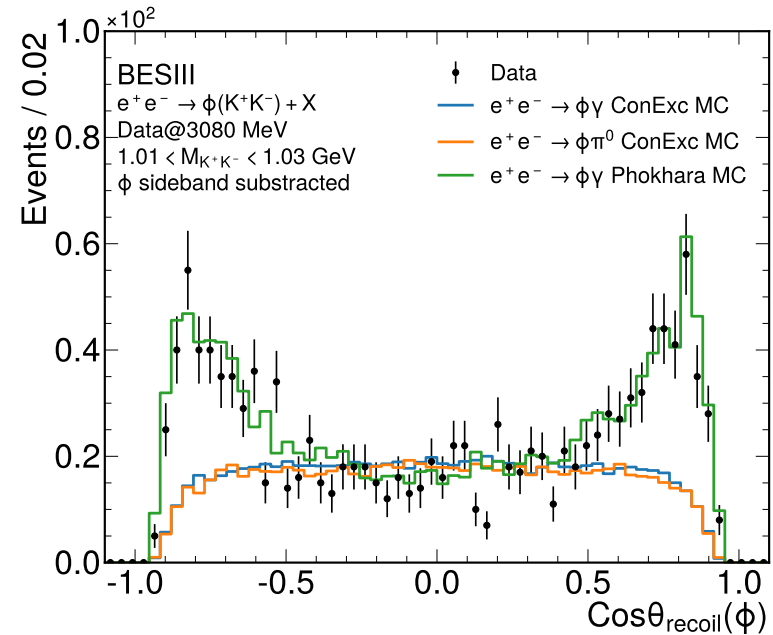
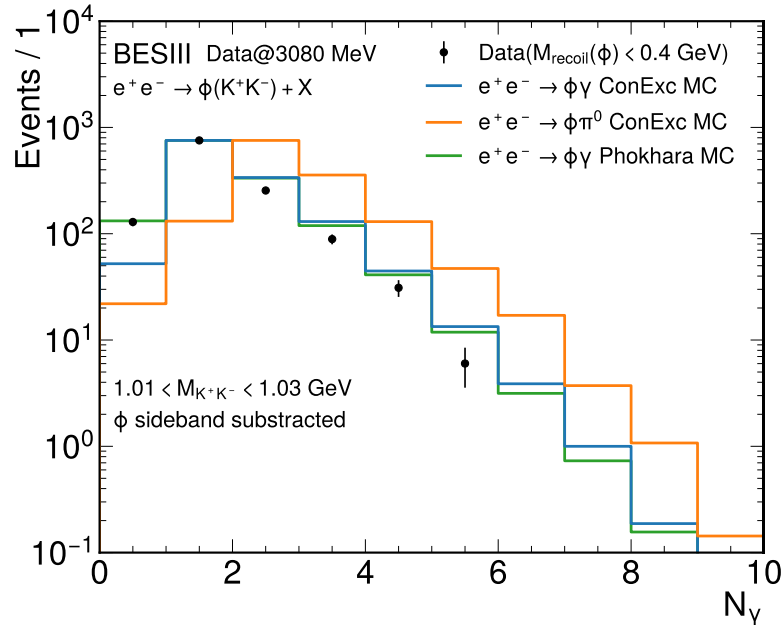
- A mass spectra fitting on the distribution of $M_{\gamma\gamma}$ is performed to determine the numbers of $e^+e^- \rightarrow \phi\pi^0$ and $e^+e^- \rightarrow \phi\gamma$.



- Almost all of events (>99.99%) in the region of $M_{recoil}(\phi) < 0.4$ GeV are from $e^+e^- \rightarrow \phi\gamma$ from the fitting results.
- An additional fit is used to distinguish if the photons are ISR photons or not.

N_γ and $\cos\theta_{recoil}(\phi)$ in $M_{recoil}(\phi) < 0.4$ GeV region

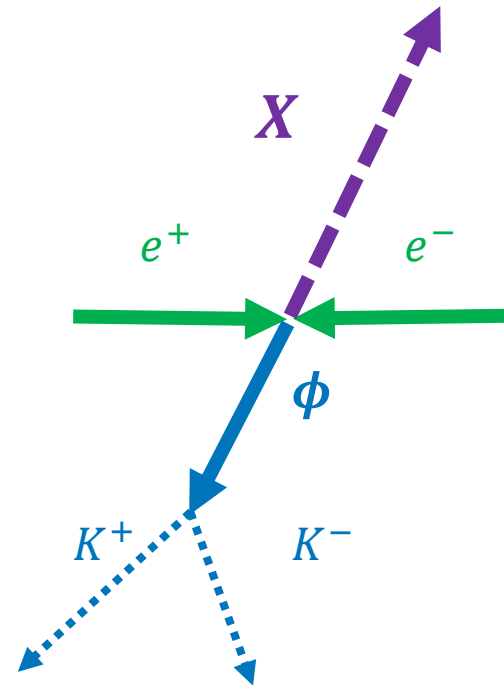
- The distributions of N_γ and $\cos\theta_{recoil}(\phi)$ for the events in the region of $M_{recoil}(\phi) < 0.4$ GeV.



- The Phokhara MC could describe the data better than the other two MC samples for both N_γ and $\cos\theta_{recoil}(\phi)$, which are related to each other.
- A simultaneous fit to N_γ and $\cos\theta_{recoil}(\phi)$ is performed.

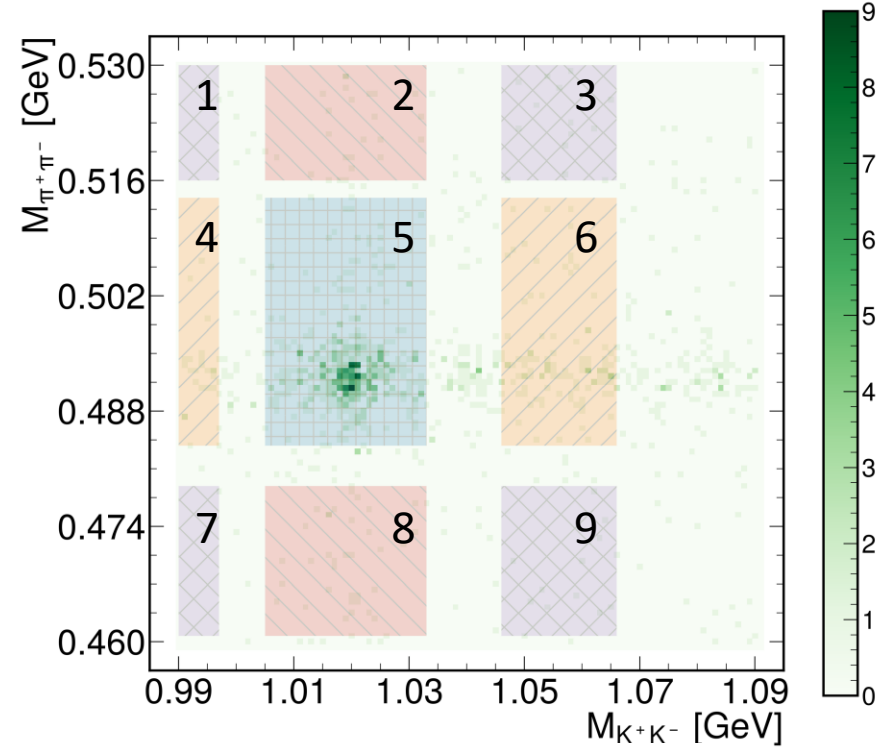
Preliminary results

- Boss version : 708.
- Data : e^+e^- collision data @3080 MeV.
- MC samples:
 - Inclusive MC : same statistic with data
 - $e^+e^- \rightarrow \phi + \pi^0$ with ConExc generator,
 - $e^+e^- \rightarrow \phi + \gamma$ with ConExc generator,
 - $e^+e^- \rightarrow \phi + \gamma$ with Phokhara generator,



2D sideband method for $e^+e^- \rightarrow \phi K_S^0 + X_2$

- ϕ and K_S^0 signal region, $1.01 < M_{K^+K^-} < 1.03$ and $0.485 < M_{\pi^+\pi^-} < 0.515$ GeV, which is highlighted with green box.
- ϕ side-band and K_S^0 signal regions, $0.990 < M_{K^+K^-} < 0.997 \cup 1.046 < M_{K^+K^-} < 1.066$ and $0.485 < M_{\pi^+\pi^-} < 0.515$ GeV, which are highlighted with black boxes.
- ϕ signal and K_S^0 side-band regions, $1.01 < M_{K^+K^-} < 1.03$ and $0.461 < M_{K^+K^-} < 0.478 \cup 0.516 < M_{K^+K^-} < 0.529$ GeV, which are highlighted with red boxes.
- ϕ side-band and K_S^0 side-band regions, $0.990 < M_{K^+K^-} < 0.997 \cup 1.046 < M_{K^+K^-} < 1.066$ and $0.461 < M_{K^+K^-} < 0.478 \cup 0.516 < M_{K^+K^-} < 0.529$ GeV, which are highlighted with purple boxes.



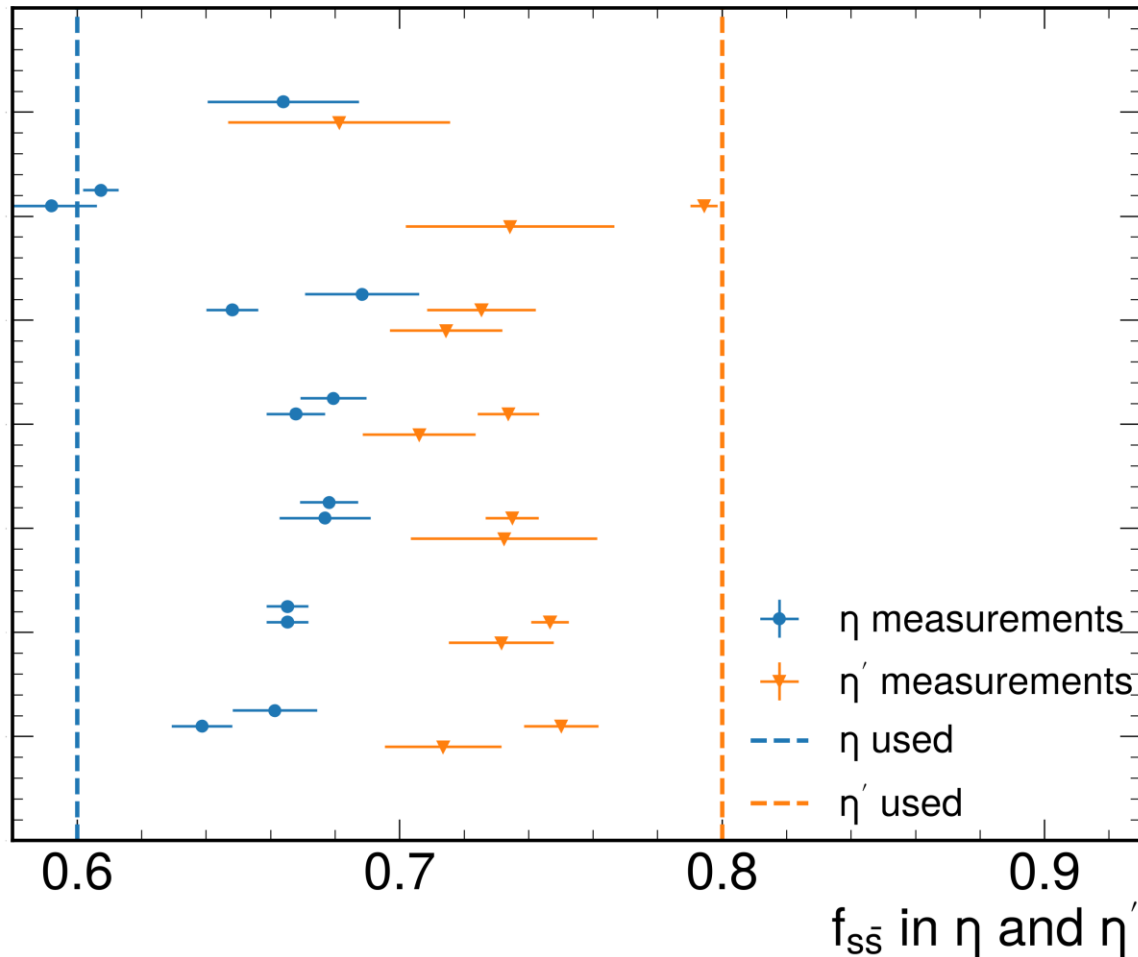
$$\omega_h = \frac{f(a, 5)}{f(a, 4) + f(a, 6)} = 0.6661$$

$$\omega_v = \frac{f(b, 5)}{f(b, 2) + f(b, 8)} = 0.5000$$

$$\omega_d = \frac{f(c, 5) - \omega_h \times (f(c, 4) + f(c, 6)) - \omega_v \times (f(c, 2) + f(c, 8))}{f(c, 1) + f(c, 3) + f(c, 7) + f(c, 9)} = -0.3331$$

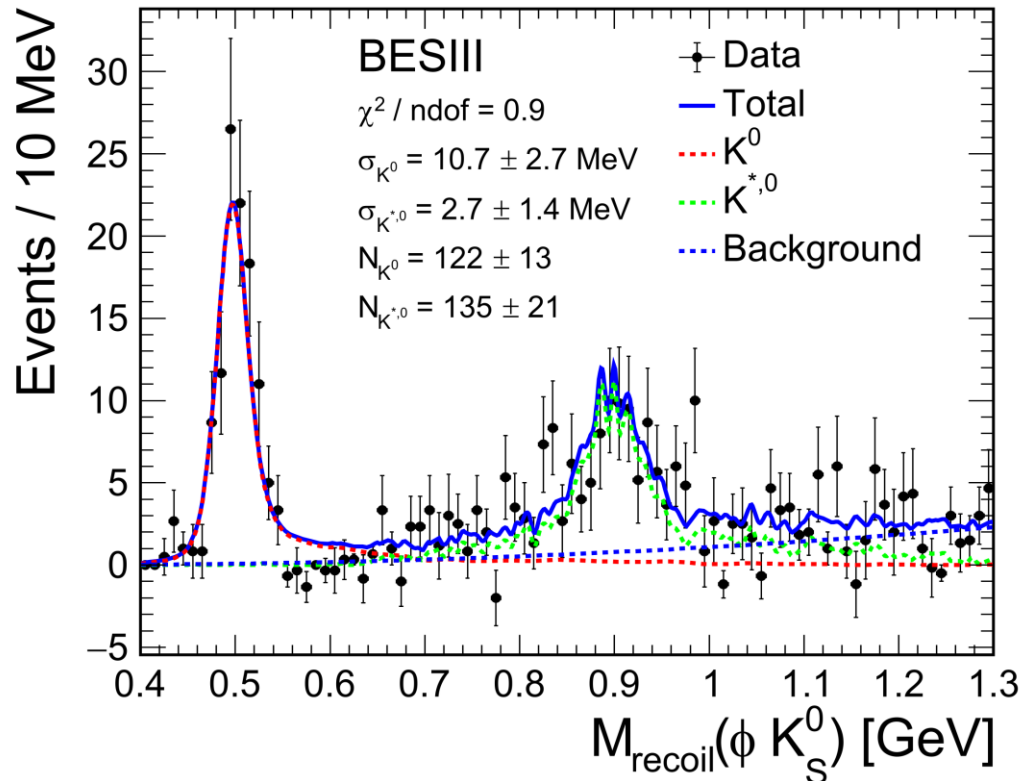
$\eta \sim \eta'$ mixing angle

➤ The mixing angle between η and η' is $(37.4 \pm 0.4)^\circ$ from [link](#).



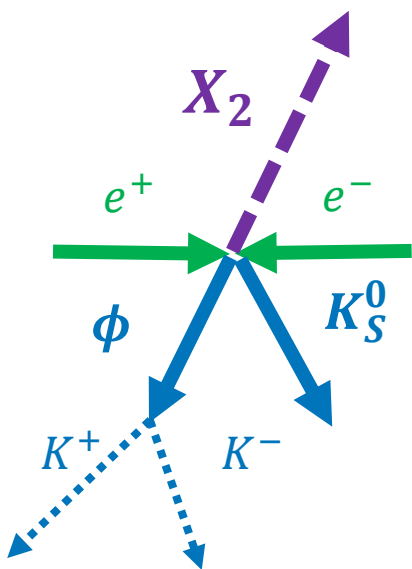
Fit results of $M_{recoil}(\phi + K_S^0 + X)$

- The fit results of M_{recoil} against ϕK_S^0 , where the signal is described by MC shape \otimes gaussian and the background is described by 2nd order polynomial.



Preliminary results of $e^+e^- \rightarrow \phi K_S^0 + X_2$

- The K_S^0 is reconstructed using $\pi^+\pi^-$ decay mode, that causes the non- K_S^0 background, such as $e^+e^- \rightarrow \phi\pi^+\pi^-\pi^+\pi^-$.
- We perform 2D mass spectra fit of $M_{K^+K^-}$ VS $M_{\pi^+\pi^-}$ to estimate the **non- K_S^0** and **non- ϕ** backgrounds.



Components	$M_{K^+K^-}$	$M_{\pi^+\pi^-}$
ϕ and K_S^0	Breit-Wigner \otimes Gaussian	Breit-Wigner \otimes Gaussian
Non- ϕ and K_S^0	2nd Chebyshev	Breit-Wigner \otimes Gaussian
ϕ and non- K_S^0	Breit-Wigner \otimes Gaussian	2nd Chebyshev
Non- ϕ and non- K_S^0	2nd Chebyshev	2nd Chebyshev

